Supporting Information

Relocation of Cobalt Ions in Electrochemically Delithiated $LiCoPO_4$ Cathode Materials

Quang Duc Truong*[,†], Murukanahally K. Devaraju[†], Yoshikazu Sasaki[‡], Hiroshi Hyodo[†], Takaaki Tomai[†], Itaru Honma*[,†]

[†]Institute of Multidisciplinary Research for Advanced Materials, Tohoku University, Sendai 980-8577, Japan.

[‡]DATUM Solution Business Operations, JEOL Ltd., Tokyo 196-0022, Japan.

Corresponding Author:

*Email: tqduc@mail.tagen.tohoku.ac.jp (Q.D.T); i.honma@tagen.tohoku.ac.jp (I.H)

ABSTRACT: Understanding the dynamic structural change during the charge/discharge cycle in cathode materials is critical for the development of high energy density battery. Here, we demonstrate directly, by aberration-corrected scanning transmission electron microscopy (STEM), that upon the electrochemical delithiation of olivine lithium cobalt phosphates, cobalt ions diffuse from M2 sites and occupy vacancy at M1 sites. The finding provides the intrinsic evidence for the capacity fading of $LiCoPO_4$ cathode materials.

Experimental section

$LiCoPO_4$ materials were synthesized by a sol-gel method according to our previous report with changing annealing temperature (Truong, Q. D.; Devaraju, M. K.; Tomai, T.; Honma, I. *ACS Appl. Mater. Interfaces* **2013**, *5*, 9926−9932). Typically, $LiNO_3$, $Co(NO_3)_2$, $NH_4H_2PO_4$, and citric acid ($C_6H_8O_7$) in a 1:1:1:1 molar ratio were dissolved in distilled water. After complete dissolution of starting materials, the obtained solution was heated with continuous stirring at 80 °C for 2 h then the hot plate temperature was set at 120 °C. After 12 h reaction, a gel-like specimens resin was obtained. For pretreatment of samples, the gel-like matter was subjected to pyrolysis at 350 °C for 2 h in air atmosphere. The resulting carbonate precursor was calcinated at 750 °C for 5 h in air and the $LiCoPO_4$ particles were obtained.

The crystalline phase of the samples were characterized using powder X-ray diffraction (XRD; Rigaku, SmartLab, 45 kV and 200 mA) with CuKα radiation (λ = 1.5406 Å). Data were collected in the 2θ-θ scanning mode with a scan speed of 2° min^{-1} and a step size of 0.02°. High Resolution TEM, HAADF, ABF imaging were conducted using JEOL JEM-2100F, Japan at 200 kV equipped with a spherical aberration corrector (CEOS). Camera length is 6 cm; BF aperture is 3 cm and HAADF, ABF detectors spanned the range of 70 to 180 mrad, 12 to 24 mrad, respectively. The background noise of the raw HAADF images were eliminate by filtering with 2D difference filters (HREM Research Inc., Japan) for obtaining images in Figure 1c and Figure 4a.

The electrochemical performance of $LiCoPO_4$ was investigated using coin-type cells (CR2032). The working electrodes is composed of 80 wt.% $LiCoPO_4$, 10 wt.% PTFE (poly(tetrafluoroethylene)) as a binder and 10 wt.% acetylene black. These materials were ground by conventional agar motor to make electrode paste. The prepared paste was spread uniformly, rolling into sheet then dried in a vacuum oven for 4 h at 160 °C. The cathode sheet was punched into circular discs and cut into wafers (7 mm in diameter, 0.025mm in thickness, 5-6 mg). The tested cell was assembled inside an argon-filled glove box. For electrochemical measurements, the cell is composed of lithium metal counter, reference electrodes and a $LiCoPO_4$ positive electrode. The cathode and reference electrodes were separated by a microporous polypropylene film. 1 M solution of $LiPF_6$ in a mixed solvent of ethylene carbonate (EC) and dimethyl carbonate (DMC) with 1:1 in volume ratio (Tomiyama Pure Chemical Co., Ltd.) was used as the electrolyte. The charge-discharge cycling were performed galvanostatically between 3.0 and 5.1 V *versus* Li/Li^+ on multi-channel battery testers (Hokuto Denko, Japan) at various charge/discharge rates ranging from 0.1 to 1 C (1 C=167mA h g^{-1}). Current densities and specific capacities were calculated on the basis of the weight of $LiCoPO_4$ cathode in the electrode.

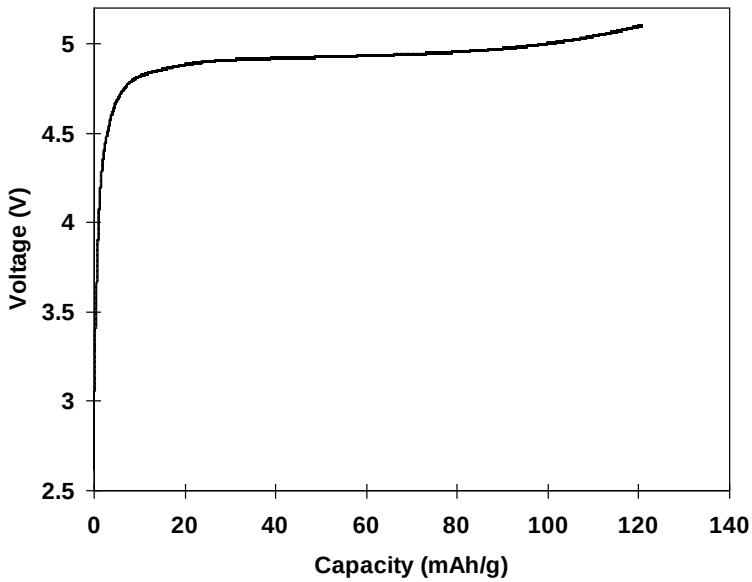

Figure S1. Charge profile of $LiCoPO_4$ sample used for STEM analysis.

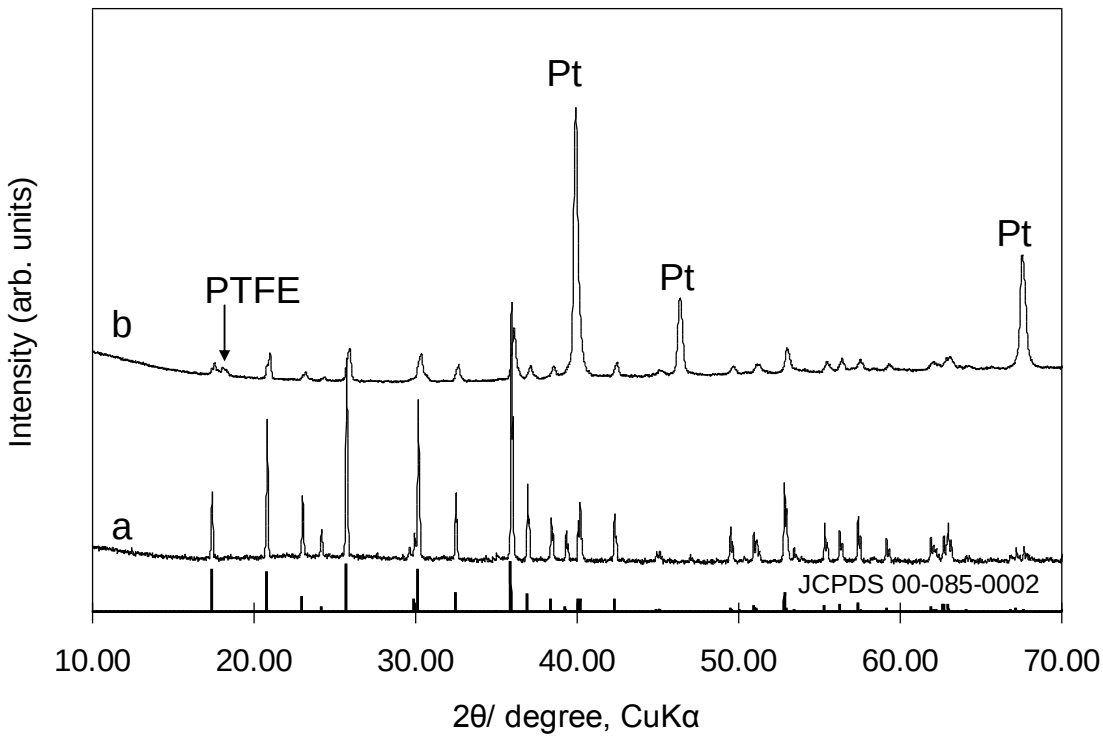

Figure S2. XRD patterns of the (a) original and (b) delithiated $Li_{1-x}CoPO_4$ samples. The most intensive peaks are ascribed to Pt current collector.

Table S1. Structural parameters obtained by Rietveld refinement.

Atom	$LiCoPO_4$				$Li_{1-x}CoPO_4$			
	x/a	y/b	z/c	B (Å^2)	x/a	y/b	z/c	B (Å^2)
Li	0.5	0.5	0.5	1	0.5	0.5	0.5	1
Co	0.2790(2)	0.25	0.9777(6)	0.5	0.2781(5)	0.25	0.991(2)	0.5
P	0.0948(4)	0.25	0.4212(9)	1	0.0932(10)	0.25	0.450(3)	1
O(1)	0.0913(9)	0.25	0.7505(16)	1	0.086(3)	0.25	0.799(4)	1
O(2)	0.4514(11)	0.25	0.2210(17)	1	0.459(3)	0.25	0.215(4)	1
O(3)	0.1616(8)	0.0484(9)	0.2798(10)	1	0.181(2)	0.049(2)	0.309(3)	1

$LiCoPO_4$

Cell parameter: a = 10.2046(2) Å, b = 5.92294(11) Å, c = 4.70099(10) Å, V = 284.134(9) Å^3.

Rietveld reliability factors: R_{WP}=2.16%, R_B=9.40%.

$Li_{1-x}CoPO_4$

Cell parameter: a = 10.1841(13) Å, b = 5.9113(7) Å, c = 4.6958(7) Å, V = 282.69(6) Å^3.

Rietveld reliability factors: R_{WP}=4.83%, R_B($Li_{1-x}CoPO_4$)=4.80%, R_B(Pt)=5.48%.

For $Li_{1-x}CoPO_4$, we measured the XRD pattern of the electrode. Thus, the peaks of PTFE and Pt were simultaneously observed. We ignored the PTFE since the peak intensity of it was very weak and performed the two phase analysis ($Li_{1-x}CoPO_4$ and Pt).

The occupancies of all atoms were fixed to 1. The atomic displacement parameters of Li, Co, P and O were fixed as values in the literature (N. N. Bramnik, K. G. Bramnik, T. Buhrmester, C. Baehtz, H. Ehrenberg and H. Fuess, *J. Solid State Electrochem.* **2004**, 8, 558-564). That of Pt was fixed to 0.5. The lattice constant of Pt was fixed to 3.922 Å.

The delithiated sample prepared at 5.1 V was unstable, may degrade partly and the sample was also contained other component of the electrode.

The Rietveld method was used to analyze the XRD patterns with the program RIETAN-FP (F. Izumi, K. Momma, *Solid State Phenom.* **2007**, 130, 15–20).

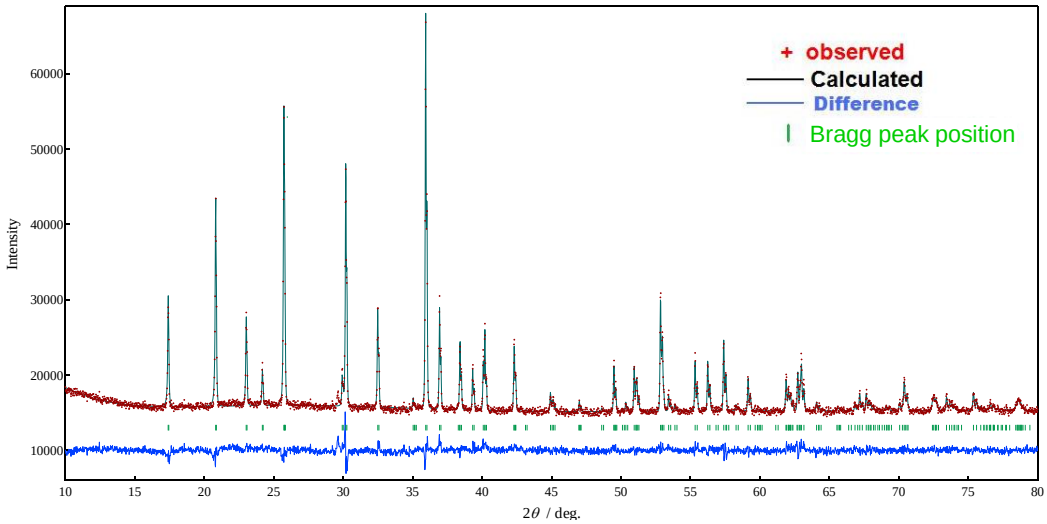

Figure S3. Experimentally acquired (+ signs) and Rietveld-calculated (solid line) X-ray diffractograms for the origin $LiCoPO_4$ sample. The differences between the experimental and calculated intensities are plotted underneath the diffractogram. The vertical tick marks between the two curves indicate Bragg reflection positions.

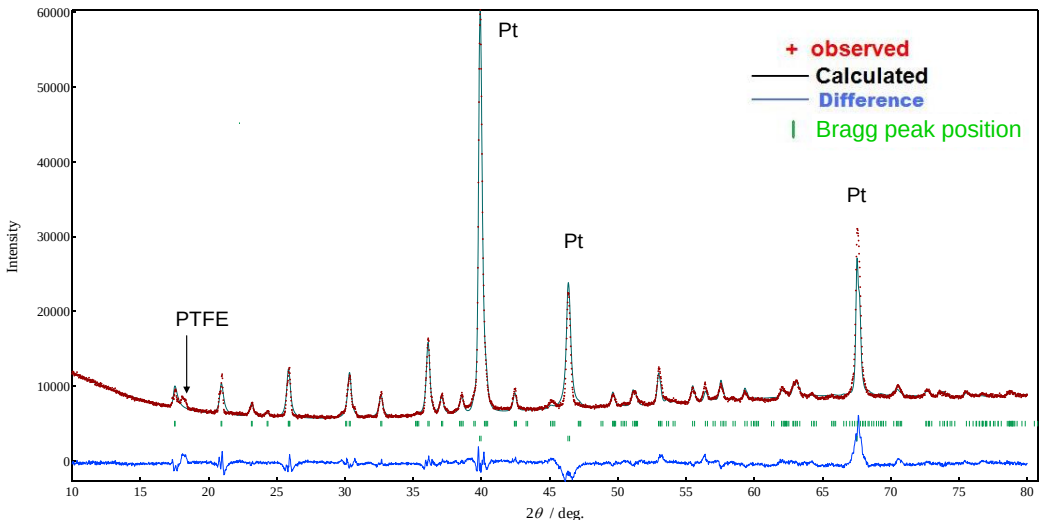

Figure S4. Experimentally acquired (+ signs) and Rietveld-calculated (solid line) X-ray diffractograms for the delithiated $Li_{1-x}CoPO_4$ sample. The differences between the experimental and calculated intensities are plotted underneath the diffractogram. The vertical tick marks between the two curves indicate Bragg reflection positions.

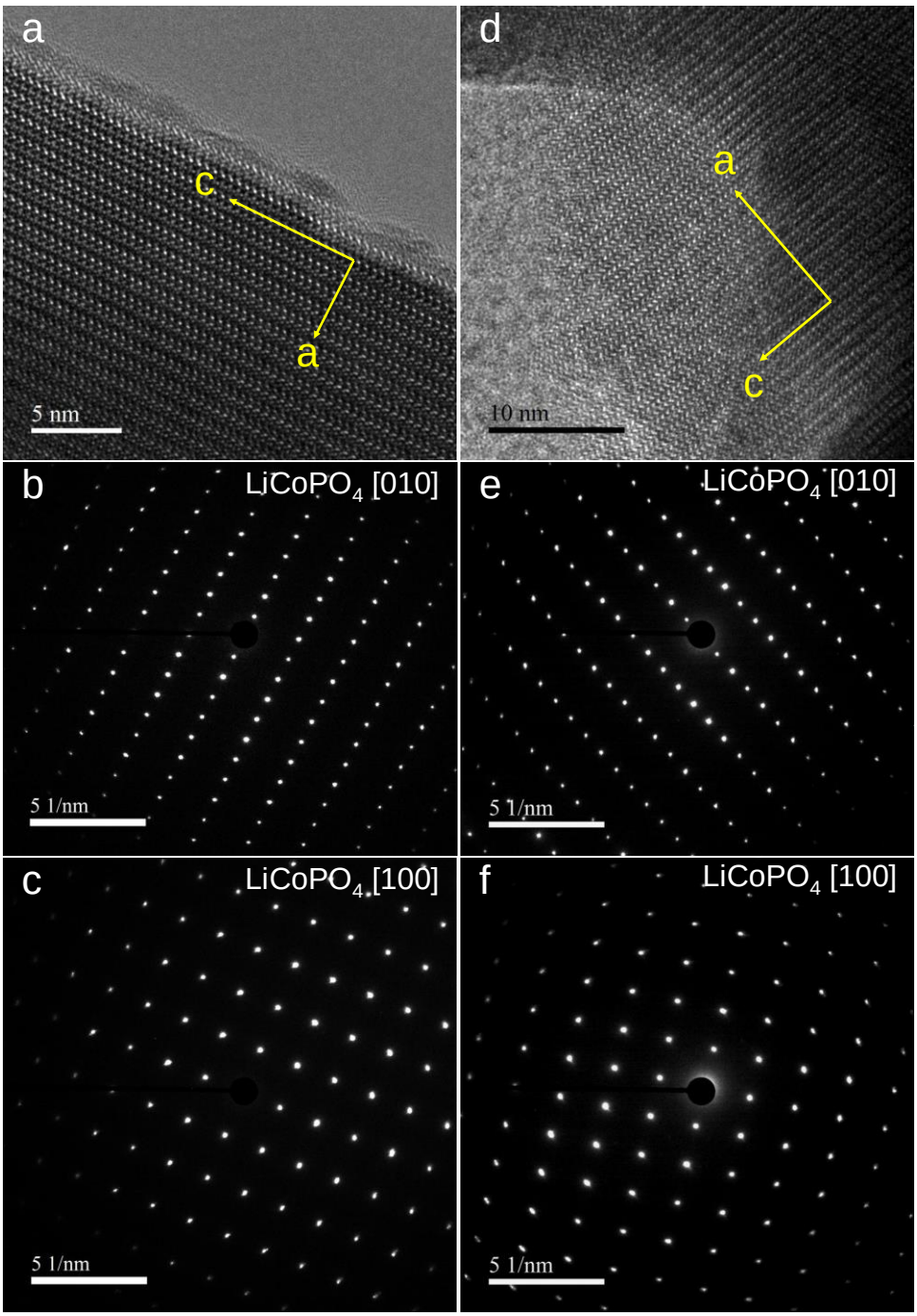

Figure S5. (a, d) HRTEM images and (b, c, e, d) corresponding SAED patterns of the (a, b, c) original and (d, e, f) delithiated $Li_{1-x}CoPO_4$ samples.

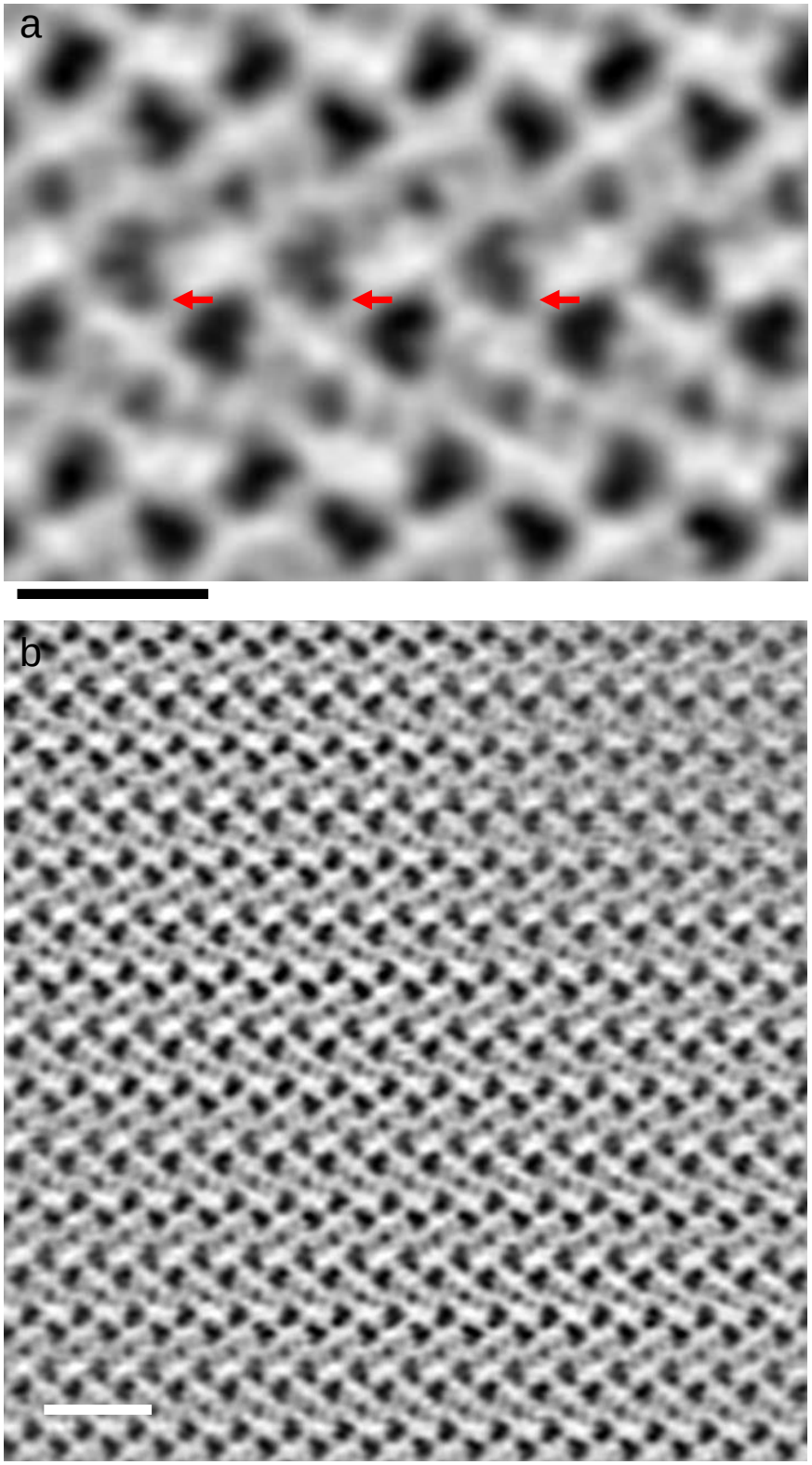

Figure S6. ABF-STEM images of the delithiated $Li_{1-x}CoPO_4$ sample: (a) Zoomed-in image with the red arrows indicate the Co column with faint contrast, the sale bars = 5 Å and (b) low magnification image shows the strong contrast at Co sites remained in large observed area, the scale bar = 1 nm.

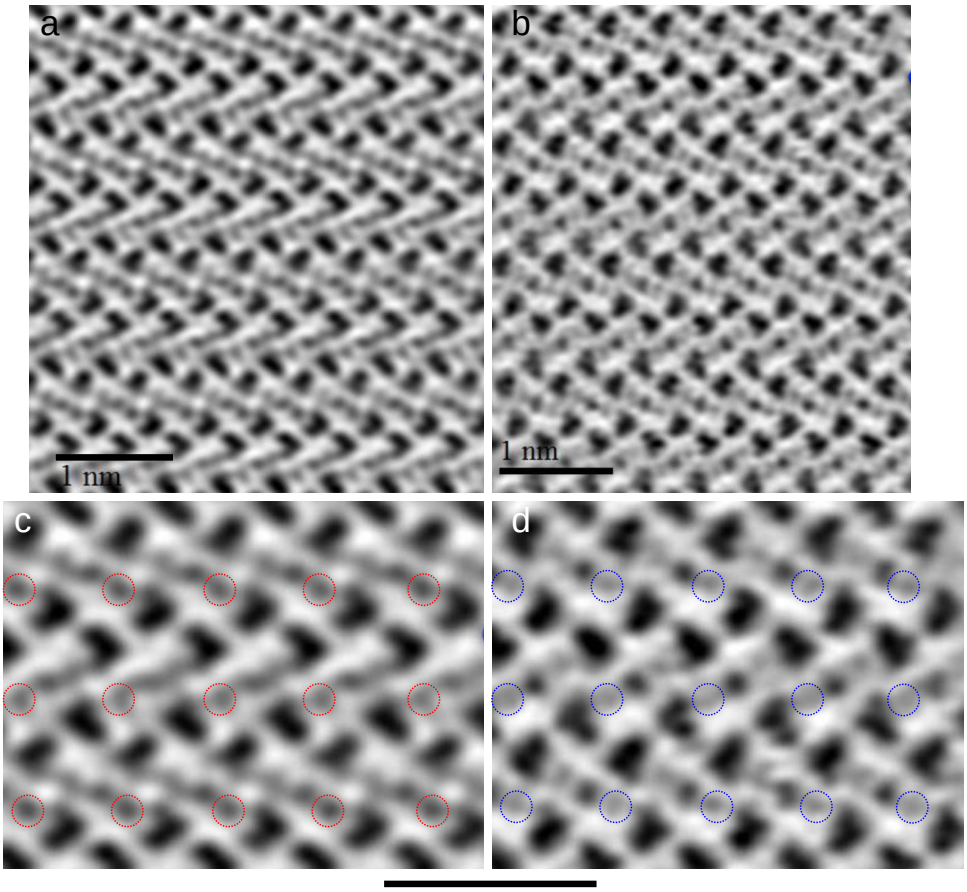

Figure S7. ABF-STEM images of the (a, c) original and (b, d) delithiated $Li_{1-x}CoPO_4$ samples, the scale bar = 1 nm. O columns are marked by red circles and the diffused O columns with the fairly low intensities in delithiated sample are marked by blue circles.

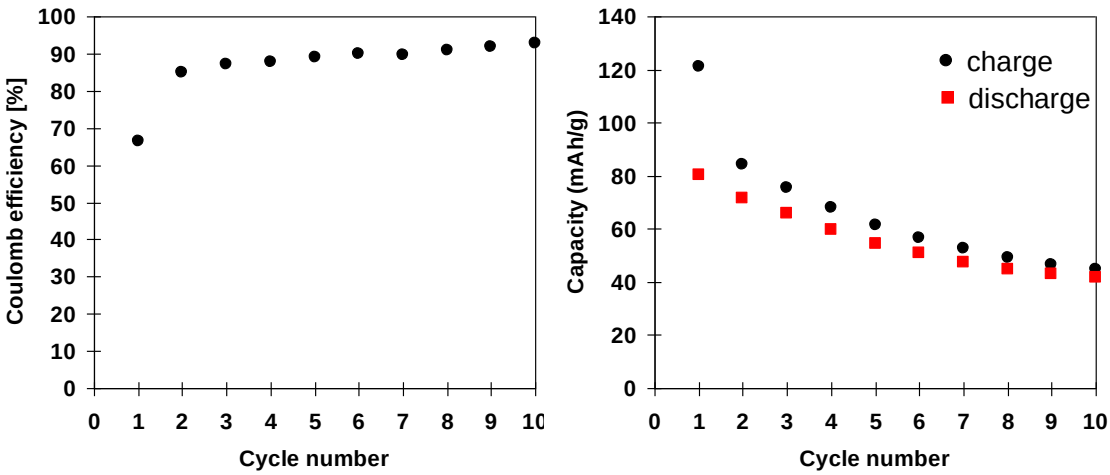

Figure S8. The coulomb efficiency and charge/discharge capacity *vs.* cycle number of the $LiCoPO_4$ sample.

Discussions

The strong and uniform contrasts observed in Li columns in this study suggest that the relocation of Co ions to M1 sites (both Co-to-Li exchange antisite defects and vacancy V_{Li} occupation) is profound in the electrochemically delithiated $Li_{1-x}CoPO_4$. Chung *et al.* demonstrated that the migration of metal ions from M2 sites to M1 sites is thermodynamically unfavorable due to the stronger electrostatic repulsion between neighboring cations at edge-sharing M1 sites.[1–3] The exchange defects would not commonly present in the lattice of $LiFePO_4$ and $LiMnPO_4$. In the present case, the formation of homogeneously distributed Co ions in the lattice can be possible explained by the formation of a new stable phases having the same olivine-like structure such as $Li_{0.7}CoPO_4$ and $CoPO_4$.[4] Such a phase would be stable with replacement of Li by Co atom without the distortion of the olivine-type structure. The phenomena is intrinsic properties of $LiCoPO_4$ material and may hinder the cathode from fast intercalation reaction.

Recently, it was suggested that the diffusion constant of ions moving in one-dimensional channels is determined by size of particle having point defects.[5] In nanosized materials, very few number of defects are presented, allowing all sites accessible by very rapid migration of Li^+ through the channels.[5] Thus, down-sizing $LiCoPO_4$ particles can be efficient to alleviate the negative effect of cobalt relocation and improve the electrochemical performance. Furthermore, lithium ions diffuse along the *b* axis very fast during the intercalation reaction. Thus, nanosheets or nanoplates with shortening of Li ion diffusion distance along [010] direction are enable to diminish the effects of antisite defects.[6–8] Further study would also be directed to minimize the metal ions relocation by optimizing the synthetic techniques, layer coating or introducing dopants to stabilize the crystal structure.

References

(1) Chung, S. Y.; Choi, S. Y.; Yamamoto, T.; Ikuhara, Y. *Phys. Rev. Lett.* **2008**, *100*, 125502.

(2) Chung, S. Y.; Choi, S. Y.; Yamamoto, T.; Ikuhara, Y. *Angew. Chem. Int. Ed.* **2009**, *48*, 543–546.

(3) Chung, S. Y.; Choi, S. Y.; Lee, S. S.; Ikuhara, Y. *Phys. Rev. Lett.* **2012**, *108*, 195501.

(4) Bramnik, N. N.; Nikolowski, K.; Baehtz, C.; Bramnik, K. G.; Ehrenberg, H. *Chem. Mater.* **2007**, *19*, 908–915.

(5) Malik, R.; Burch, D.; Bazant, M.; Ceder, G. *Nano Lett.* **2010**, *10*, 4123−4127.

(6) Truong, Q. D.; Devaraju, M. K.; Ganbe, Y.; Tomai, T.; Honma, I. *Sci. Rep.* **2014**, *4*, 3975.
(7) Rui, X; Zhao, X.; Lu, Z.; Tan, H.; Sim, D.; Hng, H. H.; Yazami, R.; Lim, T. M.; Yan, Q. *ACS Nano*, **2013**, *7*, 5637–5646.
(8) Zhao, Y.; Peng, L.; Liu, B.; Yu, G. *Nano Lett.* **2014**, DOI: 10.1021/nl5008568.